

A Dynamic Process Model for Predicting Workload in an Air Traffic Controller Task

Martina Truschinski (mtru@hrz.tu-chemnitz.de)

Department of Automation Technology
Technische Universität Chemnitz
Chemnitz, Germany

Maria Wirzberger (wirm@hrz.tu-chemnitz.de)

Department of E-Learning and New Media
Technische Universität Chemnitz
Chemnitz, Germany

Abstract

We present a dynamic process model for workload, developed according to a conducted experiment, which recorded the pupil dilation during an air traffic controller simulation. We describe how we built such a dynamic system based on the collected data. Logged events that happened in our simulation were used as system input and the recorded pupil dilation as output. Afterwards, we used the MATLAB system identification toolbox to identify the transfer function between input and output. The identified model is validated with a validation data set that has been excluded from the identification process. Results show that we are able to explain nearly 50% of the variance of the recorded pupil dilation data in the air traffic controller simulation. Moreover, the model explains some contrary results of the statistical analysis from our experiment.

Keywords: Dynamic process model; System theory; Workload; Pupillometry; Air traffic controllers

Introduction

According to current statistics, the amount of airline passengers will continue its positive development over the next years, with expected annual growth rates of up to five percent (IATA, 2017; Boeing, 2017). To maintain the resulting needs and ensure smooth and safe traveling, the duty of air traffic controllers (ATCs) is of high importance. However, tasks like this are rather complex and put high demands on the available resources of such job holders (Mogford, Guttman, Morrow, & Kopardekar, 1995). Beyond this, it is proven that predefined factors like traffic volume or frequency congestion influence ATCs' mental workload (Mogford et al., 1995).

As discussed by Gopher and Donchin (1986), the concept of mental workload enfolds various dimensions and facets. Although it has been broadly inspected, deriving a clear definition forms a rather difficult matter. Nevertheless, there are two constituting aspects that build a common ground in most cases. While task difficulty results from the demands required to successfully solve a task in a given time (Galy, Cariou, & Mélan, 2012), resource supply refers to the information processing capacity available for this purpose. In this vein, mental workload comprises the difference between required capacities of the information processing system to achieve satisfying task performance and available capacity at a given time (Gopher & Donchin, 1986; Wickens, 2008). Based on the assumption that tasks with increased difficulty require additional resources, a significant decrease in performance due

to the lack of resources should appear as soon as resource demands exceed resource supply (Wickens, G., Banbury, & Parasuraman, 2013).

There are different possibilities to estimate human workload (Prewett, Johnson, Saboe, Elliott, & Coovert, 2010; Beatty & Lucero-Wagoner, 2000; Reiner & Gelfeld, 2014) and build workload models (Gopher & Braune, 1984; Wickens, 2008). Beatty and Lucero-Wagoner (2000) described nonreflexive phasic pupillary movements as indicators for brain processes that underlie dynamic, intensive aspects of human cognition. In several research investigating the cognitive functions, task-evoked responses of the pupil (TERPs) (Beatty, 1982; Beatty & Lucero-Wagoner, 2000) were used to measure cognitive effort, workload and cognitive load (Haapalainen, Kim, Forlizzi, & Dey, 2010; Wierwille, 1979; Paas, Tuovinen, Tabbers, & Van Gerven, 2003). Therefore, in our approach we used the measured TERPs to model and validate a dynamic workload model to investigate and simulate workload in ATC tasks.

Experiment

We collected data from 25 volunteers located at the campus of University Pompeu Fabra ($M_{Age} = 28.12$; $SD = 5.67$, 64% male). The majority of 84% participants had no prior experience in ATC tasks (including, but not limited to, video games).

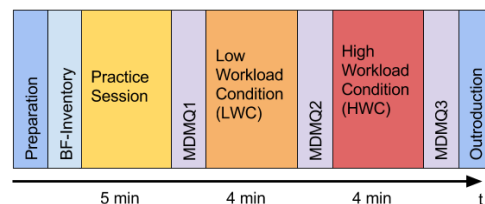


Figure 1: Experimental procedure with preparation phase, practice session and two different conditions. Measures on personality (BFI) and mood (MDMQ) are not reported in this paper.

Experimental Design

In our 2 (workload condition) x 3 (events) within-subjects design, each participant completed a simulated ATC task. The simulation was divided into a practice session and two conditions of 4 min, a low workload condition (LWC) with a lower degree of difficulty and a high workload condition (HWC) with a higher degree of difficulty. In the LWC, participants had to manage and control less airplanes appearing at a lower frequency (airplanes appeared every 4–8 s). This results in an easy task difficulty with lower time pressure, since participants had more time to handle each airplane. In the HWC, participants had to manage a greater number of airplanes appearing in a higher frequency (airplanes appeared every 1–5 s), which resulted in higher task difficulty and time pressure to avoid collisions between airplanes.

Workload Measurement Since Beatty and Lucero-Wagoner (2000) reported a significant increase in pupil dilation due to an increase in workload, we recorded the pupillary response during each condition. We used the mobile eye tracking headset from *Pupil Labs* with a sample rate of 60 Hz and analyzed the TERPs by calculating the mean pupil dilation during an 1.5 s window for three classes of events that were assumed to trigger an increase in workload. The time window of 1.5 s was chosen in line with Beatty and Lucero-Wagoner (2000), who identified that TERPs are recognized due to an increase in mental workload between 1-2 s after the presentation of a stimulus.

One class of events included all collisions caused by the participant, another one included participants actions of changing height or direction of an airplane. The third class of events included system-induced occurrences of a new couple of airplanes. All events were logged by a self-programmed protocol system, which was part of the simulated scenario. The obtained log files included timestamps for each pupillary response, which were sent to the system via a wlan-connection, as well as simultaneously recorded timestamps for each event occurrence.

Procedure

The study was conducted in a virtual reality room, called XIM, and participants were recruited directly from the campus plaza. After completing the consent forms, they were invited to enter the XIM. For each participant, the experiment started with a preparation phase, where the eye tracking glasses were put on, the Big Five Inventory (BFI) was completed and some instructions regarding the virtual reality room were given (see Figure 1). In addition, there was a calibration phase that also ensured stable light conditions with and without planes presented on the screen. Afterwards, the practice session started, in which participants received an instruction on how to structure their commands to change airplane routes (see Fig. 2) and how to avoid collisions between airplanes. Following this instructions, participants had to manage the airplanes appearing at the screen on their own.



Figure 2: Experimental setup with eye-tracking device.

This section was finished as soon as participants were able to manage the scenario, measured by 10 correct answers in a row. After the practice section, participants were exposed to two trial sections presented in static order, the LWC followed by the HWC.

In each section, the airspace was divided in several airspace areas, whereof the subjects were responsible for the middle airspace (green rectangle). At a predefined frequency (HWC: 1–5 s; LWC: 4–8 s) two airplanes with a given number and a random height appeared from both sides or from top and down heading to the same randomized point in the responsible airspace. During the whole experiment, participants had to keep in mind that airplanes, which do not collide in a 3D space, could appear at the same screen location due to the 2D display. This indirect 3D perception demands information processing resources as well (Wickens et al., 2013), but since all participants were exposed to comparable requirements, we did not expect additional effects on the measured level of workload. For avoiding collisions, participants had to use control commands with a similar structure compared to real ATC commands (see Figure 3). In detail, they had to provide to the number of the chosen airplane plus the information about what they want to change, for instance the direction or height of the airplane. The experimenter in the back adopted the role of the pilot, controlling the airplanes by sending special keyboard sequences to the simulation. Each session comprised a break as well. During this time span, participants reported their mood state by completing the Multi-dimensional Mood State Questionnaire (MDMQ). After finishing the LWC and HWC, the experimenter removed the eye tracker glasses.

Data Analysis and Model Preparation

After conducting the experiment and preparing the pupil dilation data, we analyzed the data statistically and computed a dynamic model of workload over the task with an identified and fitted dynamic system (Isermann & Münchhof, 2011). With reference to the latter, we developed some hypothetical assumptions based on the curve progressions of figure 6 in Beatty (1982). We assumed that dealing with appearing airplanes and setting a command will increase participants' workload (see Fig. 4). If a collision happened, we expected participants to immediately recognize their mistake and think about. However, at the same time the complexity of the air space should be reduced due to the reduced number of air

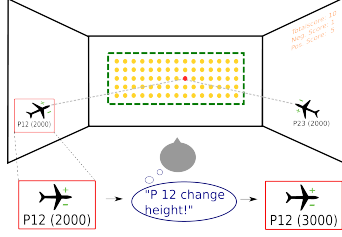


Figure 3: Schematic representation how participants had to change the height of an airplane.

planes on the screen. On this account, we assumed an initial increase in workload after collisions, directly followed by a decrease caused by the reduced amount of airplanes.

Data preparation

To calculate the mean pupil dilation, the recorded data had to be cleaned from artifacts, blinks and other undesired patterns in the data stream (Beatty & Lucero-Wagoner, 2000). Therefore, we used MATLAB-functions to implement standard methods for cleaning and analyzing pupil dilation data. First, we deleted all blinks in the signal, which are characterized by zero values in the data stream. Then, we interpolated the missing values and used a median filter in order to clean the signal from outliers. Participants with more than 18% blinks or zeros in the data stream were excluded from the statistical analysis, as the filtering functions and the evaluation could be falsified by very noisy signals. For the statistical approach, we calculated the respective level of workload for the events "collision", "disappear" and "appear" as mean of all occurred TERPs *after* the system had logged the collision or the appearance of airplanes. Due to the fact that our simulation only recognized if an airplane changed its direction or height, we measured the level of workload for the event "action" from TERPs calculated during an 1.5 s window *before* the change happened. Within our statistical analyses, we calculated the mean of the pupil dilation of LWC and HWC as measure of workload for the particular condition.

Statistical Results

We conducted a repeated measures analysis of variance (ANOVA), to validate TERPs as predictor for workload. Event ("collision" vs. "appear" vs. "disappear") and workload condition (LWC vs. HWC) were regarded as independent variables and the recorded TERPs as indicator of workload were defined as dependent variable. Mauchly's test indicated a violation in the assumption of sphericity for the main effect of event, $\chi^2(5) = 73.049, p < .001$, as well as the interaction between condition and event, $\chi^2(5) = 42.331, p < .001$, thus degrees of freedom were corrected using Greenhouse-Geisser estimates of sphericity for event, $\epsilon = .388$, and the interaction, $\epsilon = .573$. We found a significant main effect for event, $F(1.17, 19.79) = 12.394, p < .05, \eta_p^2 = 0.42$, but no significant main effect of workload condition. Post-hoc pairwise comparisons with Bonferroni correction

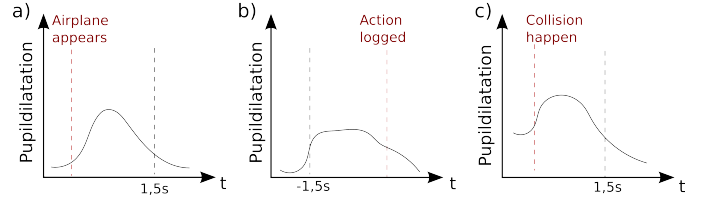


Figure 4: Assumed schematic curve progression of TERPs during different events.

pointed out that the workload after an action ($p < .001$) and after a collision ($p < .05$) was significantly higher than the average workload in the whole condition. However, the workload after the appearance of an airplane was significantly lower ($p < .05$). Moreover, a significant interaction effect between condition and event showed up, $F(1.72, 29.24) = 3.701, p < .05, \eta_p^2 = .18$, indicating a difference in the workload between events in both conditions. Since we had a static order, the level of workload in the HWC could have been influenced by the LWC. To control for this effect, we computed pupil dilation means during a 1 s window at the beginning of the LWC and HWC and conducted a paired-samples t-test. It did not show significant results, $t(19) = -1.927, p > .05$, thus we can assume that there was no influence on workload evoked by the static order.

Workload Model

We assume that different levels of workload in both conditions result from task difficulty and the different events corresponding to the behavior of simulation and participants. Therefore, each simulated event as well as the spoken commands should have a direct influence on the level of workload in each condition, resulting in different TERPs. Thus, in the dynamic approach, the pupil dilation as level of workload is described as output that is dependent on the events, which are described as inputs. If there was a stable unique relation between input and output, we should be able to find a mathematical model for the temporal behavior of the workload (TERPs) from the measured input of the events.

System Description

In system theory, such model can be described as multiple input and single output model (MISO), at which appearance, disappearance and collisions of airplanes as well as actions commanded by the participants are inputs, whereas the obtained TERPs are regarded as output. In detail, we measured a continuous time signal, with pupillary response and the related events as impulse responses appearing in each condition. An impulse response can be defined as the output of a process being excited by an impulse ($\delta(s)$) (Isermann & Münchhof, 2011).

$$\delta(t) = \begin{cases} \infty & \text{for } t = 0 \\ 0 & \text{for } t \neq 0 \end{cases} \quad (1)$$

For a better understanding, while the step response or impulse response can be measured easily in many cases, we modeled our input events as step functions, whereas a step ($\sigma(s)$) can be obtained by integrating the impulse with respect to time t (Isermann & Münchhof, 2011).

$$\sigma(t) = \begin{cases} 1 & \text{for } t \geq 0 \\ 0 & \text{for } t < 0 \end{cases} \quad (2)$$

To estimate important system parameters, such as settling time or the the damping coefficient and other characteristic values, we can use the following generic transfer function

$$G(s) = \frac{y(s)}{u(s)} = \frac{b_0 + b_1(s) + b_{m-1}(s)^{m-1} + b_m(s)^m}{a_0 + a_1(s) + a_{m-1}(s)^{m-1} + a_m(s)^m} \quad (3)$$

which is the Laplace transformation of an ordinary differential equation (ODE) for a lumped parameter system (for further details see Isermann and Münchhof). Since we model our input data with step responses, we can directly take some individual characteristic values from the calculated step response of the system, which might be used to determine coefficients of special transfer functions by means of simple calculations (Isermann & Münchhof, 2011). With the system identification toolbox, MATLAB offers a great database of identification methods to solve such process identification problems. Therefore, we used MATLAB to identify our workload model based on the data we collected during the experiment.

Modeling the input For modeling the system input, we used the timestamps of appearances and disappearances of airplanes as well as collisions and actions within the tasks from participants' log files. Based on this, we created several time series for each event class, which contained a step response at each event timestamp recorded by the simulation. Since airplanes stayed on the screen till they disappeared, we had to take into account that appearance and disappearance of airplanes have a different influence on the resulting workload compared to commands and collisions. Thus, the σ -function of appear is increased by two if an airplane couple appeared on the screen and the σ -function of disappear is increased by the number of airplanes which left the air space unharmed. By contrast, the influence of actions and collisions lasted only a limited time (an action during the time the participant spoke and the collision as long as the collision sound was played and the airplanes disappeared). Therefore, the σ -function of action was set to 1 for the time frame of 2 s before an action happened (see Fig. 5(a)). We chose these time window because the middle duration of commands was 2 s. Due to the fact that an airplane collision reported relatively short by a collision sound, we modeled the σ -function of collision by setting it to 1 for the time frame of 1 s after a collision happened (see Figure 5(b)).

Identify the types of transfer functions for events After modeling the input, we analyzed the behavior of the pupil

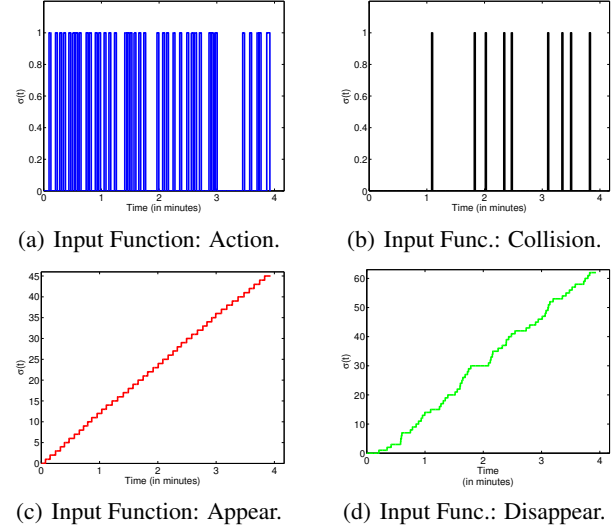


Figure 5: Example step response function of all events.

dilation over 4 s time windows during the recorded events. The chosen time windows doubled the recommended 2 s time window (Beatty & Lucero-Wagoner, 2000), as for identifying the dynamic of the system we had to ensure that the event-related response was included even with potential reaction time differences between participants. Moreover, the additional information of the signal behavior could help to find the right time constants.

In system theory, there exist several LTI(Linear-Time-Invariant)-systems, which describe different patterns of behavior in signals with linear ODEs. In the mathematical view, this behavior is described with the transfer function $G(s)$, which describes how a step response(s) influences the output signal. For example, a transfer function for an PT_1 -system can be described by

$$G(s) = \frac{y(s)}{u(s)} = \frac{b_0}{1 + a_1s} = K \frac{1}{1 + T_1s} \quad (4)$$

in which PT_1 -system results depend on an step response in an increase of K during the time T_1/T , whereas T is the sampling rate of the signal. Thus, the time constant T_1 describes how fast the signal reached the value K . In terms of the workload description such a system would describe how the workload will be influenced over time. Whereas T_1 describes how fast the workload is increased and K describes the absolute increase or decrease of the workload after an event is recorded. A more detailed view and the explanation of all types of LTI-systems are described in Isermann and Münchhof (2011).

Since we focused on developing a general model for each event and there might be some disturbing influences within recorded TERPs, we calculated the mean of all TERPs and regarded this as a baseline within our identification process. Such disturbing influences could be seen in miscalculated workload within overlapping, unrecognized or overwhelming events. By calculating the mean progression of the TERPs

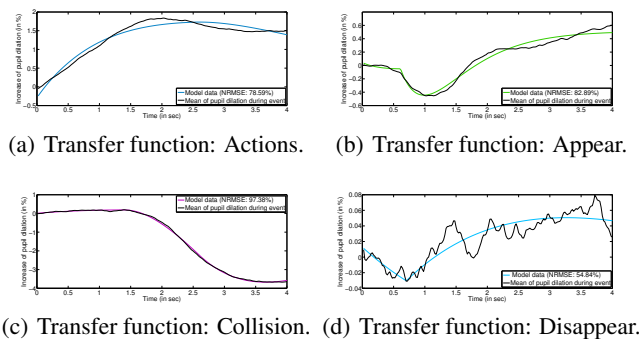


Figure 6: Curve progression of TERPs at different events.

during the events, we assume that disturbing influences might be distracted from the characteristic behavior. In Figure 6, we show the behavior of the TERPs based on this means (black lines in each figure). Moreover, it outlines that we identified transfer functions for the each step function of several events, therefore the mathematical description of our transfer function could be seen as the mathematical description of our TERPs depending on event inputs (colored lines). We identified a PT_2 -system for the action, which shows a short initial decrease in workload, followed by a steep increase. The under-damped PT_2 -system with a death time for the behavior of collision, shows that there was no significant increase in workload after a collision but a decrease after 0.5-1.0 s. The identified system of appear comprises a DT_2 -system with a death time, which shows a significant increase in workload during an spoken command. The signal of disappearance reveals that the reaction of this event is very small (signal range is between 0.08 and -0.05). Potential reasons might be the lack of reaction in pupil dilation to this event or an ineptly small size of the chosen time window for identifying a significant change. Thus, we have to handle the identified PT_2Z -system with death time carefully, since it might be incorrect. Of course, these identified models are "ideal" models to the mean behavior of the TERPs, but they can provide a hint on the type of underlying system and a clue for the range of the used time constants. Such applies in particular for collision and action, since these events are most likely to trigger direct and fast input-response behavior.

Identify the overall system behavior Based on the identified dynamic system for the TERPs, we aimed to identify the

Table 1: Identified parameters of the mean curve progression of all event-based TERPs.

System	K	T_1	T_2	T_z	T_d	T_w	ζ
Action	1.25	1.84	1.59				
Appear	.51	.52	.52	-1.4	.59		
Collision	-10	1.41				.96	.89
Disapp	-.2	4	4	-10	.66		

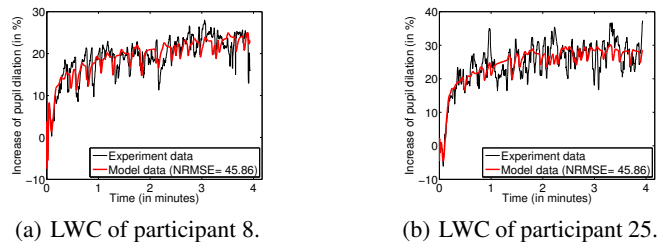


Figure 7: Comparison of recorded and modeled pupil dilation for participants 8 (training data) and 25 (validation data).

underlying dynamic system behavior of pupil dilation for the whole conditions. We assumed that the measured pupil dilation reflects the sum of responses to the input. For validating our model, we divided the data in a training data set, containing 16 participants (80% of the sample), and a validation data set, containing four participants (20% of the sample). Data of LWC and HWC were represented as independent experiments and contained the time series of the events (see Figure 5) and the corresponding recorded measurements of the pupil dilation. We defined the types of systems and their possible range of parameters detected in the TERP-analysis as system structure, to identify the complete model of pupil dilation behavior. Afterwards, we used the system identification toolbox to identify the best model describing change of pupil dilation over time depending on the event inputs. Figure 7(a) shows the simulated and the experimental output of the dynamical pupil dilatation system of two examples of the training and validation data set. We see the typical increase of the pupil dilation during the conditions of participants 8 and 25 (black lines) and the corresponding model outputs (red lines) with their exponential curve progression. The goodness-of-fit is calculated by the normalized root mean square error ($P_8 = 46.06\%$, $P_{25} = 45.68$) and shows that the peaks in the pupil dilation are the result of TERPs from actions and the dips are the result of TERPs from happened collisions. The fitted model parameters for different transfer functions are displayed in table 2. As expected, in the fitted time constants of appear and disappear event-related influences are very slow ($T_{1ap} = 104.2$; $T_{1di} = 211.2$), compared to action and collision ($T_{1ac} = 1.72$; $T_{1co} = 1.5$). Furthermore, the absolute influence of an action and a collision ($K_{ac} = 2.77$; $K_{co} = -9.58$) to the workload is greater than the appearance and disappearance of airplanes ($K_{ap} = 0.93$; $K_{di} = -1.0$).

Table 2: Identified parameters of event-based TERPs based on pupil dilation data of the whole conditions.

System	K	T_1	T_2	T_z	T_d
Action	2.77	1.72	1		
Appear	.93	104.2	.61	-.62	.6
Collision	-9.58	1.5	.96		1.14
Disappear	-1	211.2	55.65		.74

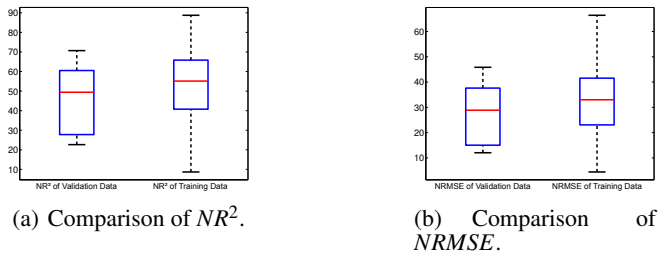


Figure 8: Comparison of experiment and fitted model data

Validation of the model The model described above was identified by data from the LWC and HWC of the first 16 participants. To measure how good our model can represent the recorded data of participants the model never seen, we calculated the deviation between model and experiment data over all participants and conditions by the normalized root mean square error (NRMSE) and the normalized coefficient of determination (NR^2). In Figure 8 shows the goodness-of-fit-results of our training data set and the validation data set. For the NRMSE, we reached mean values of 28.87% for the validation data set and 32.99% for the training data set. If we look at the NR^2 , the model is able to explain 49.42% of variance in the validation data and 55.10% in the training data.

Discussion

We developed and identified a dynamic model for the TERPs within a simulated ATC scenario. Corresponding to our expectations, statistical analyses show a significant increase in participants' TERPs due to collisions and actions, indicating metacognitive reflections about commands or mistakes. Contradictory results show up with a significant decrease in TERPs after the appearance of a couple of airplanes that afterwards increases again (see Figure 6(b)). These effects are very slow and the sole calculation of state based statistics is prone to lose this information. On this account, we built and validated a dynamic model to predict workload of ATC-Tasks based on the experimental results. We used different models for each event logged in the session, and thus can conclude that not each visual input provides the same TERPs (Beatty & Lucero-Wagoner, 2000). Furthermore, we show that the resulting workload in our condition is the sum of the responses of our system to the events. However, the increase is not a straight line, but rather an exponential increase, which might occur as well in similar experiments that investigate workload. Moreover, we can conclude that there is a stable unique relation between events in the simulation and the resulting TERPs, as we were able to find a mathematical model for the temporal behavior of the pupil dilation. Still, this model is just an approximation of the dynamic processes of workload that might be limited by the underlying linear process model. Nevertheless, we were already able to explain and predict nearly 50% of the variance in the resulting workload.

Further steps

In the next instance, we will conduct another experiment with a duration of 7 min and two conditions, an emotional and a neutral session. In this vein, we can validate our identified workload progression for the extended time frame and furthermore investigate how the emotional influence in the second condition changes the dynamics of our model. Based on these results, we will extend our model by an emotional component, simulating and predicting the influence of emotions to the workload and TERPs.

References

- Beatty, J. (1982, March). Task-evoked pupillary responses, processing load, and the structure of processing resources. *Psychological Bulletin*, *91*(2), 276–292.
- Beatty, J., & Lucero-Wagoner, B. (2000). The pupillary system. In J. T. Cacioppo, L. G. Tassinary, & G. G. Berntson (Eds.), *Handbook of Psychophysiology* (2nd ed.). Cambridge: Cambridge University Press.
- Boeing. (2017). *Estimated annual growth rates for passenger and cargo air traffic from 2016 to 2035, by region*. in *statista - the statistics portal*. Retrieved from <https://www.statista.com/statistics/269919/growth-rates-for-passenger-and-cargo-air-traffic>
- Galy, E., Cariou, M., & Mélan, C. (2012). What is the relationship between mental workload factors and cognitive load types? *International Journal of Psychophysiology*, *83*, 269–275.
- Gopher, D., & Braune, R. (1984). On the Psychophysics of Workload: Why Bother with Subjective Measures? *Human Factors: The Journal of the Human Factors and Ergonomics Society*, *26*, 519–532.
- Gopher, D., & Donchin, E. (1986). Workload - An examination of the concept. In K. R. Boff, L. Kaufmann, & J. P. Thomas (Eds.), *Handbook of Perception and Human Performance. Vol. II. Cognitive Processes and Performance*. New York: Wiley & Sons.
- Haapalainen, E., Kim, S., Forlizzi, J. F., & Dey, A. K. (2010). Psycho-Physiological Measures for Assessing Cognitive Load. Copenhagen.
- IATA. (2017). *Annual growth in global air traffic passenger demand from 2005 to 2017*. in *statista - the statistics portal*. Retrieved from <https://www.statista.com/statistics/193533/growth-of-global-air-traffic-passenger-demand>
- Isermann, R., & Münchhof, M. (2011). *Identification of Dynamic Systems*. Berlin, Heidelberg: Springer Berlin Heidelberg.
- Mogford, R. H., Guttman, J. A., Morrow, S. L., & Kopardekar, P. (1995). *The Complexity Construct in Air Traffic Control: A Review and Synthesis of the Literature*. (Tech. Rep.). DTIC Document.
- Paas, F., Tuovinen, J. E., Tabbers, H., & Van Gerven, P. W. M. (2003, March). Cognitive Load Measurement as a Means to Advance Cognitive Load Theory. *Educational Psychologist*, *38*(1), 63–71.
- Prewett, M. S., Johnson, R. C., Saboe, K. N., Elliott, L. R., & Coovert, M. D. (2010). Managing workload in humanrobot interaction: A review of empirical studies. *Computers in Human Behavior*, *26*, 840–856.
- Reiner, M., & Gelfeld, T. M. (2014). Estimating mental workload through event-related fluctuations of pupil area during a task in a virtual world. *International Journal of Psychophysiology: Official Journal of the International Organization of Psychophysiology*, *93*, 38–44.
- Wickens, C. D. (2008). Multiple Resources and Mental Workload. *Human Factors: The Journal of the Human Factors and Ergonomics Society*, *50*, 449–455.
- Wickens, C. D., G., H. J., Banbury, S., & Parasuraman, R. (2013). *Engineering psychology and human performance*. Upper Saddle River, New Jersey: Pearson Education.
- Wierwille, W. W. (1979). Physiological measures of aircrew mental workload. *Human Factors: The Journal of the Human Factors and Ergonomics Society*, *21*(5), 575–593.